Applied Radiation and Isotopes 154 (2019) 108846

Contents lists available at ScienceDirect

Applied Radiation and Isotopes

journal homepage: www.elsevier.com/locate/apradiso

Determination of k_0 and Q_0 for ^{74}Se, ^{113}In, ^{186}W and ^{191}Ir targets applying covariance analysis

L.F. Barros, R.V. Ribeiro, M.S. Dias*, M. Moralles, R. Semmler, I.M. Yamazaki, M.F. Koskinas

Instituto de Pesquisas Energéticas e Nucleares (IPEN-CNEN/SP), Centro do Reator de Pesquisas - CRPq, C.P. 11049, Pinheiros, 05422-970, São Paulo SP, Brazil

HIGHLIGHTS

- Activation parameters k_0 and Q_0 were determined for ^{74}Se, ^{113}In, ^{186}W and ^{191}Ir.
- The irradiation position was chosen where the neutron spectrum shape parameter α is very close to zero.
- All partial uncertainties and correlations between parameters were considered.

ARTICLE INFO

Keywords:
k_0 method
Gamma-ray spectrometry
Se
In
W
Ir isotopes
Neutron activation analysis
Nuclear reactor

ABSTRACT

In the present work, the determinations of k_0 and Q_0 for ^{74}Se, ^{113}In, ^{186}W and ^{191}Ir targets were performed. The irradiations were conducted near the core of the IEA-R1 4.5 MW swimming-pool nuclear research reactor of the Instituto de Pesquisas Energéticas e Nucleares (IPEN-CNEN/SP – Nuclear and Energy Research Institute), in São Paulo, Brazil. The irradiation position was chosen where the neutron spectrum shape parameter α is very close to zero. For this reason, the correction to be applied for the determination of Q_0 is very close to one, thus improving the accuracy of the results. For each experiment, two irradiations were carried out in sequence: the first one with bare samples and the second with a cadmium cover around the samples. All partial uncertainties were considered, applying the covariance matrix methodology. The final results were compared with the literature.

1. Introduction

There have been continued efforts to provide more accurate values of k_0 and Q_0 parameters in order to fulfill the Neutron Activation Analysis (NAA) user needs (e.g. Jaćimović and Stibilj, 2010; Lin and Von Gostomski, 2013; Chilian et al., 2014; Arboccò et al., 2014; Sneyers and Vermaercke, 2014; Stopic and Bennett, 2014; Trkov et al., 2015). At the same time, new statistical techniques have been introduced (Dias et al., 2010, 2011; Barros, 2018) to supply not only the overall uncertainties in these parameters but also their correlations.

In the present study, ^{74}Se, ^{113}In, ^{186}W and ^{191}Ir targets were considered. The irradiations were conducted near the core of the IEA-R1 4.5 MW swimming-pool nuclear research reactor of the Instituto de Pesquisas Energéticas e Nucleares (IPEN-CNEN/SP – Nuclear and Energy Research Institute), in São Paulo, Brazil. The irradiation position was chosen where the neutron spectrum shape parameter α is very close to zero. For this reason, the correction to be applied for the determination of Q_0 is very close to one, improving the accuracy of the results. For each experiment, two irradiations were carried out in sequence: the first with bare samples and the second with a cadmium cover around the samples.

The reason for choosing ^{74}Se was to compare the results with De Corte and Simonits (2003), Jaćimović (Jaćimović and Stibilj, 2010), k_0 Database (k_0 Database, 2019), Sneyers and Vermaercke (2014) and Lin and Von Gostomski (2013). ^{113}In was selected in order to verify the influence of overlapping wide low-energy absorption resonances, mainly for the determination of Q_0 (Kodeli and Trkov, 2007; Farina Arboccò et al., 2014); at the Second Research Coordination Meeting on the Reference Database for Neutron Activation Analysis (Firestone and Kellett, 2008) the value of k_0 for the reaction ^{186}W(n, γ)^{187}W showed a discrepancy comparing the experimental value of the resonance integral with the one calculated from differential data. ^{191}Ir was chosen following the suggestion by Stopic (Stopic and Bennett, 2014) who recommended Q_0 should be determined separately for this isotope using reactors better suited for that purpose. This is the case of the present irradiation position where α is very close to zero. All partial uncertainties were considered, applying the covariance matrix methodology.

* Corresponding author.
E-mail addresses: msdias@ipen.br, maurosilvadias@gmail.com (M.S. Dias).

https://doi.org/10.1016/j.apradiso.2019.108846
Received 14 January 2019; Received in revised form 25 July 2019; Accepted 6 August 2019
Available online 09 August 2019
0969-8043/

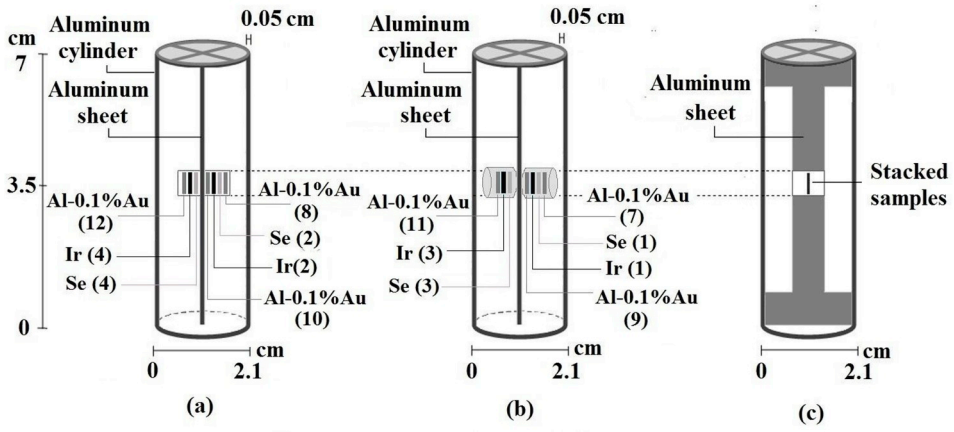

Fig. 1. Rabbits prepared for the irradiations carried out in 2016 with Au–Al, Se and Ir samples;
(a) Samples without cadmium cover; (b) Samples with cadmium cover; (c) Rabbit front view. The numbers inside parentheses correspond to the sample identification. Similar rabbits were prepared in 2015 for In, W, Zr, Co–Al and Au–Al samples.

2. Materials and methods

The parameter k_0 was obtained by the following relationship (De Corte, 1987):

$$k_{0,ij} = \frac{A_{sp,ij} - \frac{(A_{sp,ij})_{Cd}}{F_{Cd_i}} \frac{G_{th,c}}{G_{th,i}} \frac{\varepsilon_c}{\varepsilon_{ij}}}{A_{sp,c} - \frac{(A_{sp,c})_{Cd}}{F_{Cd_c}}} \text{(Method k}_0\text{ A)} \quad (1)$$

where $k_{0,ij}$ is the k_0 factor with respect to the comparator (Au) corresponding to the *i-th* reaction product and *j-th* gamma-ray; $(A_{sp,ij})_{Cd}$ and $A_{sp,ij}$ are the total absorption gamma-ray peak area of the *i-th* reaction product and *j-th* gamma-ray, with and without cadmium cover, respectively; F_{Cdi} and F_{Cdc} are the cadmium transmission factor for the target and comparator, respectively; ε_c and ε_{ij} are the peak efficiencies for the comparator and target nuclei, respectively and $G_{th,c}$ and $G_{th,i}$ are the self-shielding correction factor for thermal neutrons, for the comparator and target nuclei, respectively.

An additional formula for k_0 may be given by (De Corte, 1987):

$$k_{0,ij} = \frac{A_{sp,ij}}{A_{sp,c}} \frac{G_{th,c} \cdot f + G_{e,c}\, Q_{0,c}(\alpha)}{G_{th,i} \cdot f + G_{e,i}\, Q_{0,i}(\alpha)} \frac{\varepsilon_c}{\varepsilon_{ij}} \text{ (Method k}_0\text{ B)} \quad (2)$$

where f corresponds to the ratio between the thermal and epithermal neutron fluxes (Equation (8)).

The neutron spectrum shape parameter α may be obtained by the *Cd-covered multi-monitor method* (De Corte, 1987), measuring the slope of the curve

$$Y_i = a + \alpha X_i, \quad (3)$$

where:

$$X_i = ln\bar{E}_{r,i}$$

and

$$Y_i = ln\left[\frac{(\bar{E}_{r,i})^{-\alpha}(A_{sp,ij})_{Cd}}{k_{0,ij}\,\varepsilon_{ij}\,F_{Cd_i}\,Q_{0,i}(\alpha)\,G_{e,i}}\right] \text{(Method } \alpha \text{ A)} \quad (4)$$

In equation (3), the index *i* refers to the *i-th* target nucleus; $\bar{E}_{r,i}$ is the effective resonance energy; $(A_{sp,ij})_{Cd}$ is the total absorption gamma-ray peak area corresponding to the *i-th* reaction product and *j-th* gamma-ray, obtained by HPGe gamma-ray spectrometry measurements. The samples were irradiated with and without cadmium cover and corrected for saturation, decay time, cascade summing, geometry, measuring time and mass; $k_{0,ij}$ and ε_{ij} are respectively: the k_0 factor and gamma-ray peak efficiency corresponding to the *i-th* target nucleus and *j-th* gamma-ray; $Q_{0,i}(\alpha)$ is the ratio between the resonance integral and the thermal cross section as a function of α and $G_{e,i}$ is the self-shielding correction factor for epithermal neutrons.

An alternative technique to measure α is called *Cd-ratio multi-monitor method* (De Corte, 1987). In this case the value of Y_i is given by:

$$Y_i = ln\frac{(\bar{E}_{r,i})^{-\alpha}}{(F_{Cd_i} \cdot R_{Cd,i} - 1) \cdot Q_{0,i}(\alpha) \cdot G_{e,i}/G_{th,i}} \text{ (Method } \alpha \text{ B)} \quad (5)$$

where R_{Cdi} (Cadmium Ratio) is the ratio between A_{spij} and $(A_{spij})_{Cd}$; $G_{th,i}$ is the self-shielding correction factor for thermal neutrons.

The α value was obtained from equations (3)–(5). In the two methods described above, since the Y_i values depend on the α parameter, an iterative procedure must be performed until convergence is achieved.

The Q_0 value was calculated from $Q_0(\alpha)$ which is given by the following expression (De Corte, 1987):

$$Q_{0,i}(\alpha) = \frac{F_{Cd_c} R_{Cd,c} - 1}{F_{Cd_i} R_{Cd,i} - 1} \frac{G_{th,i}}{G_{th,c}} \frac{G_{e,c}}{G_{e,i}} \cdot Q_{0c}(\alpha) \quad (6)$$

where

$$Q_{0,i}(\alpha) = \frac{Q_{0,i} - 0.429}{(\bar{E}_{r,i})^{\alpha}} + \frac{0.429}{(2\alpha + 1)\,(0.55)^{\alpha}} \quad (7)$$

From equation (7) it can be noted that $Q_0(\alpha)$ approaches Q_0 when α goes to zero. Therefore it becomes clear the advantage of placing the samples at an irradiation position where α is close to zero, which is the case of the present work, as shown in previous works performed at the same irradiation position (Dias et al., 2010, 2011).

For the comparator (Au), $Q_{0,c}(\alpha)$ was obtained from the published value of $Q_{0,c}$ (k0 database, 2019) inserted into equation (7) and the result was applied to equation (6). For the target sample the $Q_{0,i}(\alpha)$ value was obtained first and then applied to equation (7), in order to obtain $Q_{0,i}$.

The values of effective resonance energy $\bar{E}_{r,i}$ to be applied in equations (1)–(7) were taken from (k0 database, 2019). The values of self-shielding correction factors G_{th} and G_e were calculated by code MATSSF (Trkov, 2016) except in the G_e determination for ^{186}W. For the cases of ^{74}Se and ^{113}In, which were solutions embedded in filter paper, the corrections were very small and were calculated by considering the filter paper composition and the amount of deposited material on it. In the case of ^{191}Ir, only the filter paper composition was considered, because MATSSF does not calculate the corrections for ^{191}Ir. For the case of ^{186}W the G_e correction factor was high, therefore direct measurements were performed by comparing the activity of the solid sample to the one obtained by irradiating an embedded solution with the target material on filter paper (Barros, 2018).

The parameter f, which corresponds to the ratio between the thermal and epithermal neutron fluxes, was determined by the *Cd-ratio multi-monitor method* as follows:

$$f = (F_{Cd} \cdot R_{Cd} - 1) G_e Q_0(\alpha)/G_{th} \quad (8)$$

In the present paper this parameter was determined as the average

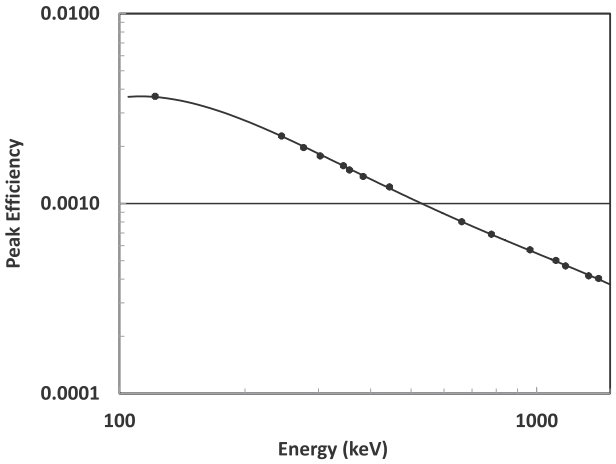

Fig. 2. Experimental HPGe peak efficiency, as a function of the gamma-ray energy. The black marks correspond to standard sources. The energy interval is 121–1408 keV.

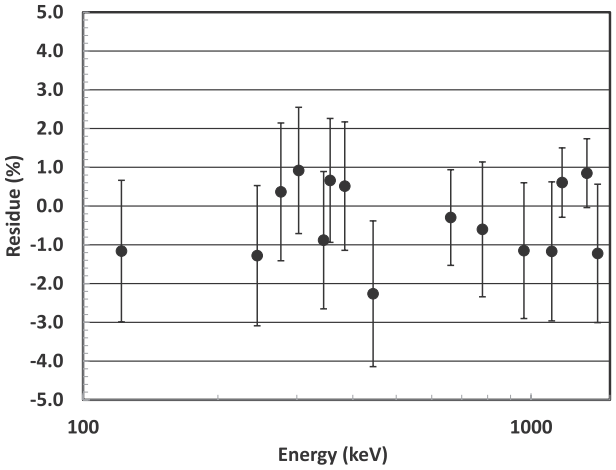

Fig. 3. Percent residues of the HPGe efficiency fitting function corresponding to a 4th degree polynomial in log-log scale. The gamma-ray energy interval is 121–1408 keV.

of all Au–Al samples used in a given experiment (pair of irradiations with and without Cd cover, as described in section 2.4).

2.1. Sample preparation and irradiation

Samples of Zirconium (*Aldrich Chemical Company,* purity 99.98%, thickness 0.25 mm), Tungsten (*Reactor Experiments*, purity 99.96%, thickness 0.15 mm), Indium (*Reactor Experiments*, purity 99.999%, diameter 0.76 mm, mass 1 mg, dissolved by nitric acid and embedded in filter paper), Selenium (*VHG Labs*, certified reference material in solution), Iridium (*SPEX Plasma Standards*, certified reference material in solution), alloys of Au (0.10% in Al, IRMM–530RC) and Co (0.475% in Al, Reactor Experiments Inc.) were used in the irradiations. All masses were measured accurately by a Mettler Toledo XP56 microbalance and the samples were placed in the irradiation position 24A, near the 4.5 MW IEA-R1 reactor core. In this position, the parameter α was previously measured to be very small (Dias et al., 2010). The samples were wrapped with thin aluminum foils and positioned in the middle of a cylindrical aluminum container (*rabbit*) 7.0 cm long, 2.1 cm in diameter and 0.05 cm thick. In order to compensate for the neutron flux gradient along the distance from the rabbit axis, positioned parallel to the reactor core, each sample was sandwiched within a pair of Au samples which were used as monitors of neutron flux variation. The samples were irradiated in duplicate, one at each side of an aluminum rectangular sheet used to mount them inside the rabbit, as shown in Fig. 1. In this way, up to six Au–Al samples were irradiated together with the target samples in each rabbit.

Two sets of rabbits were prepared for each experiment: one with a cadmium cover around the samples and the other without it. These sets were irradiated during 60 min each, in sequence: the first without cadmium cover and the second with it. The minimum decay time before measurements was around 24 h. During 2015 the selected targets for k_0 determination were W and In. For the irradiations in 2016 the selected targets were In, Se and Ir. The α curves were determined by the conventional methods (equations (4) and (5)) and used ^{197}Au, ^{59}Co, ^{94}Zr and ^{96}Zr monitors.

2.2. Efficiency calibration

Standard sources of ^{60}Co, ^{133}Ba, ^{137}Cs and ^{152}Eu, traceable to a

Table 2
Values obtained for G_{th}, G_e and F_{Cd}; the numbers inside parentheses are the uncertainties in the last digits (one standard deviation).

Target	G_{th}	G_e	F_{Cd}[a]
^{59}Co	0.9984(3)	0.990(2)	0.990(2)
^{74}Se	0.9953(11)	0.9999(1)	0.872(26)
^{94}Zr	0.9981(4)	0.972(6)	0.999(1)
^{96}Zr	0.9981(4)	0.966(6)	0.997(2)
^{113}In	0.9912(2)	0.9995(1)	0.986(3)
^{186}W	0.959(8)	0.390(11)	0.990(2)
^{191}Ir	0.9953(11)	0.9999(1)	0.78(2)[b]
^{197}Au	0.9990(2)	0.9956(9)	0.998(1)

[a] Trkov et al, 2015.

Table 3
Values obtained for f and α by different methods. Method *A* corresponds to the *"Cd-covered multi-monitor method"*; Method *B* corresponds to the *"Cd-ratio multi-monitor method"*;. The numbers inside parentheses correspond to uncertainties in the last digits (one standard deviation).

Year	Method	f	Year	Method	α ($\times 10^{-3}$)
2015	B	45.0(1)	2015–2016	A	−3.5(87)
2016	B	46.0(1)	2015–2016	B	−2.5(64)
2016	B	42.3(9)	Average		−3.1(47)

Table 1
Parameters and Correlation Matrix of the efficiency curve fitting obtained in 2015. The fitted function was: $ln(\varepsilon) = a_0 + a_1[ln(E/E_0)] + a_2[ln(E/E_0)]^2 + a_3[ln(E/E_0)]^3 + a_4[ln(E/E_0)]^4$ and $E_0 = 800$ keV.

Parameter		Absolute Uncertainty	Correlation Matrix (× 1000)				
a_0	−7.314	6.7×10^{-3}	1000				
a_1	-9.24×10^{-1}	1.3×10^{-2}	−81	1000			
a_2	8.30×10^{-2}	1.4×10^{-2}	−454	−141	1000		
a_3	-8.24×10^{-2}	3.1×10^{-2}	−128	−854	538	1000	
a_4	-7.11×10^{-2}	1.3×10^{-2}	−41	−889	365	979	1000
χ^2/ν	1.03						

Table 4:
Results obtained for k_0 by different methods. Method *A* corresponds to the *"Cd-ratio multi-monitor method"*; Method *B* corresponds to the *"Cd-covered multi-monitor method"*. The numbers inside parentheses correspond to uncertainties in the last digits (one standard deviation). The references are indicated by a superscript and are described at the bottom of the table.

Reaction	Gamma Energy (keV)	Method A	Method B	Weighted Average	Literature (indicated as superscript)			
$^{74}Se(n,\gamma)\ ^{75}Se$	121.12	$2.16(5) \times 10^{-3}$	$2.17(4) \times 10^{-3}$	$2.17(4) \times 10^{-3}$	$1.94(1) \times 10^{-3}$ [a]	$2.19(3) \times 10^{-3}$ [b]	$2.18(3) \times 10^{-3}$ [c]	$2.18(5) \times 10^{-3}$ [d]	$2.14(4) \times 10^{-3}$ [e]
	136.00	$7.49(14) \times 10^{-3}$	$7.54(13) \times 10^{-3}$	$7.52(13) \times 10^{-3}$	$6.76(7) \times 10^{-3}$ [a]	$7.14(14) \times 10^{-3}$ [b]	$7.33(9) \times 10^{-3}$ [c]	$7.44(19) \times 10^{-3}$ [d]	$7.32(13) \times 10^{-3}$ [e]
	264.66	$7.57(14) \times 10^{-3}$	$7.58(12) \times 10^{-3}$	$7.58(12) \times 10^{-3}$	$7.11(5) \times 10^{-3}$ [a]	$7.57(14) \times 10^{-3}$ [b]	$7.53(9) \times 10^{-3}$ [c]	$7.52(19) \times 10^{-3}$ [d]	$7.39(13) \times 10^{-3}$ [e]
	279.54	$3.16(7) \times 10^{-3}$	$3.22(5) \times 10^{-3}$	$3.19(5) \times 10^{-3}$	$3.00(4) \times 10^{-3}$ [a]	$3.19(12) \times 10^{-3}$ [b]	$3.18(4) \times 10^{-3}$ [c]	$3.19(8) \times 10^{-3}$ [d]	$3.14(6) \times 10^{-3}$ [e]
	400.66	$1.49(5) \times 10^{-3}$	$1.52(4) \times 10^{-3}$	$1.51(4) \times 10^{-3}$	$1.43(1) \times 10^{-3}$ [a]	$1.38(2) \times 10^{-3}$ [b]	$1.44(2) \times 10^{-3}$ [c]	$1.45(4) \times 10^{-3}$ [d]	$1.435(3) \times 10^{-3}$ [e]
$^{113}In(n,\gamma)^{114m}In$	190.30	$1.019(18) \times 10^{-3}$	$1.024(18) \times 10^{-3}$	$1.021(16) \times 10^{-3}$	$1.06(1) \times 10^{-3}$ [a,c]	$1.02(1) \times 10^{-3}$ [f]			
	558.40	$2.71(6) \times 10^{-4}$	$2.74(5) \times 10^{-4}$	$2.73(5) \times 10^{-4}$	$2.86(2) \times 10^{-4}$ [a, c]	$2.70(3) \times 10^{-4}$ [f]			
	725.20	$2.71(7) \times 10^{-4}$	$2.74(5) \times 10^{-4}$	$2.73(5) \times 10^{-4}$	$2.90(2) \times 10^{-4}$ [a, c]	$2.70(3) \times 10^{-4}$ [f]			
$^{186}W(n,\gamma)^{187}W$	479.53	$3.23(8) \times 10^{-2}$	$3.21(8) \times 10^{-2}$	$3.22(8) \times 10^{-2}$	$2.97(3) \times 10^{-2}$ [a, c]				
	551.53	$7.34(19) \times 10^{-3}$	$7.30(18) \times 10^{-3}$	$7.31(18) \times 10^{-3}$	$6.91(3) \times 10^{-3}$ [a, c]				
	618.77	$9.18(24) \times 10^{-3}$	$9.13(22) \times 10^{-3}$	$9.15(22) \times 10^{-3}$	$8.65(4) \times 10^{-3}$ [a, c]				
	625.51	$1.59(5) \times 10^{-3}$	$1.58(5) \times 10^{-3}$	$1.58(5) \times 10^{-3}$	n.r. [a, c]				
	685.77	$3.99(10) \times 10^{-2}$	$3.96(9) \times 10^{-2}$	$3.97(9) \times 10^{-2}$	$3.71(2) \times 10^{-2}$ [a, c]				
	772.89	$6.00(16) \times 10^{-3}$	$5.97(14) \times 10^{-3}$	$5.98(15) \times 10^{-3}$	$5.61(4) \times 10^{-3}$ [a, c]				
$^{191}Ir(n,\gamma)^{192}Ir$	295.96	1.170(17)	1.167(19)	1.169(18)	1.15(2) [g1]	1.13(2) [g2]	1.137(14) [c]	1.134(15) [h]	
	308.46	1.197(17)	1.172(19)	1.186(18)	1.15(2) [g1]	1.19(2) [g2]	1.176(14) [c]	1.174(18) [h]	
	316.51	3.38(5)	3.36(5)	3.37(5)	3.30(4) [g1]	3.23(4) [g2]	3.26(4) [c]	3.253(39) [h]	
	468.07	1.949(30)	1.948(33)	1.949(31)	1.91(2) [g1]	1.85(2) [g2]	1.874(26) [c]	1.870(14) [h]	

The numbers inside parentheses are the uncertainties in the last digits (one standard deviation). [a] De Corte and Simonits (2003); [b] Jaćimović and Stibilj (2010); [c] k0 database (2019); [d] Sneyers and Vermaercke (2014); [e] Lin and Von Gostomski (2013); [f] Arboccò et al. (2014); [g1]Chilian et al. (2014) – *Polytechnique*; [g2]Chilian et al. (2014) – SCK•CEN; [h]Stopic and Bennett (2014); n.r. not reported.

Table 5
Comparison between the k_0 and the literature, applying the Zeta score parameter. Agreement was considered for Zeta below 3.0 (99% confidence interval). The references are indicated by a superscript and are described at the bottom of the table.

Reaction	Gamma Energy (keV)	Zeta Score between pairs of k_0 values obtained in this work and from the literature (indicated as superscript)				
$^{74}Se(n,\gamma)\ ^{75}Se$	121.12	5.52[a]	−0.40[b]	−0.21[c]	−0.18[d]	0.53[e]
	136.00	4.87[a]	1.83[b]	1.02[c]	0.25[d]	0.92[e]
	264.66	3.54[a]	0.00[b]	0.27[c]	0.26[d]	1.00[e]
	279.54	2.60[a]	−0.23[b]	−0.31[c]	−0.38[d]	0.26[e]
	400.66	1.94[a]	2.91[b]	1.57[c]	1.06[d]	1.87[e]
$^{113}In(n,\gamma)^{114m}In$	190.30	−2.07[a,c]	0.05[f]			
	558.40	−2.41[a,c]	0.10[f]			
	725.20	−3.16[a,c]	0.10[f]			
$^{186}W(n,\gamma)^{187}W$	479.53	2.93[a,c]				
	551.53	2.19[a,c]				
	618.77	2.24[a,c]				
	625.51	–				
	685.77	2.74[a,c]				
	772.89	2.38[a,c]				
$^{191}Ir(n,\gamma)^{192}Ir$	295.96	0.74[g1]	1.49[g2]	1.45[c]	1.54[h]	
	308.46	1.34[g1]	−0.15[g2]	0.44[c]	0.47[h]	
	316.51	1.09[g1]	2.19[g2]	1.72[c]	1.85[h]	
	468.07	1.06[g1]	2.68[g2]	1.85[c]	2.32[h]	

[a] De Corte and Simonits (2003).
[b] Jaćimović and Stibilj (2010).
[c] k0 database (2019).
[d] Sneyers and Vermaercke (2014).
[e] Lin and Von Gostomski (2013).
[f] Arboccò et al. (2014).
[g1] Chilian et al. (2014) – *Polytechnique*.
[g2] Chilian et al. (2014) – SCK•CEN.
[h] Stopic and Bennett (2014).

$4\pi\beta-\gamma$ absolute counting system installed at the LMN, were used for obtaining the HPGe gamma-ray peak efficiency as a function of the energy. These sources were sealed inside a 0.022 cm polyethylene plus 0.052 cm aluminum capsule and were positioned 17.9 cm away from the crystal front face. The peak area was calculated applying a linear background function under the peak and summing the counts in the region of interest, selected from $-1.5 \times$ FWHM to $+1.5 \times$ FWHM, where FWHM is the Full Width at Half Maximum of the total energy absorption peak.

An accurate pulser was introduced in the gamma-ray spectrum close to the right edge, in order to perform dead time and pile-up corrections. A fourth degree polynomial in log-log scale was fitted between the HPGe peak efficiency and the normalized gamma-ray energy, E/E_0, where E_0 is an arbitrary energy (800 keV), chosen to reduce the uncertainty in the interpolation (Dias et al., 2004) and covering the 121 keV–1408 keV energy range. The uncertainty in the interpolated efficiency was in the 0.9% to 2.2% range.

In order to verify the accuracy in the ranges between 121-244 keV and 661–778 keV, where there are no experimental points, Monte Carlo simulations were applied using MCNP6 with optimized source-detector dimensions, based on the experimental points from other energy regions. The results of efficiency ratios between the comparator (Au) and the target reaction products, comparing all experimental and calculated efficiencies, indicated a good agreement, with an average difference around 0.4%. Considering this result, the experimental efficiency curve was adopted as it contains all correlations between points. Two efficiency curves were determined: one in 2015 and another one in 2016. Both yielded similar results.

Table 6
Results obtained for Q_0. The numbers inside parentheses correspond to uncertainties in the last digits (one standard deviation). The references are indicated by a superscript and are described at the bottom of the table.

Reaction	Q_0						
	Present Work	Literature (indicated as superscript)					
^{74}Se(n,γ) ^{75}Se	11.3(6)	10.8(7) [a]	9.81(10) [b]	11.0(3) [c]	11.2(3) [d]	11.175 [e]	
^{113}In(n,γ)^{114m}In	24.7(6)	24.2(4) [a, c]				27.88 [e]	23.7(5) [f]
^{186}W(n,γ)^{187}W	12.9 (6)	13.7(2) [a, c]				12.75 [e]	
^{191}Ir(n,γ)^{192}Ir	3.77(11)	3.94(20) [g1]	3.47(10) [g2]	3.7(3) [c]			

The numbers inside parentheses are the uncertainties in the last digits (one standard deviation). [a] De Corte and Simonits (2003); [b]Jaćimović and Stibilj (2010); [c] k0 database (2019); [d]Sneyers and Vermaercke (2014); [e]Trkov et al., 2015; [f] Arboccò et al. (2014); [g1]Chilian et al. (2014) – *Polytechnique*; [g2]Chilian et al. (2014) – SCK•CEN.

2.3. Covariance matrix methodology

The discussion on the covariance methodology applied to the conventional formalism has been presented in our previous papers (Dias et al., 2010, 2011).

3. Results and discussion

The behavior of the experimental peak efficiency as a function of the gamma-ray energy for the HPGe spectrometer, conducted in 2015 is presented in Fig. 2. The results indicated in black marks correspond to experimental points. The continuous line corresponds to a 4th degree polynomial fit in log-log scale. The percent residues are presented in Fig. 3 and showed good agreement within the experimental uncertainties. The parameters associated with the fitting are shown in Table 1. The reduced Chi-Square value was 1.03 indicating a satisfactory fit. The results of efficiency obtained in 2016 were very similar to ones obtained in 2015.

The cascade summing correction was below 1.8% with an uncertainty of less than 0.2%. The results of G_{th}, G_e are shown in Table 2 and were calculated as described in section 2. The F_{Cd} was taken from Trkov et al., 2015), except for ^{191}Ir, which was taken as the average values from Chilian et al., 2014). The results of f and α are specific to the selected irradiation position and are shown in Table 3. The value of f may change from time to time due to the presence of absorbing materials in the nearby positions. The value of α turned out to be less sensitive to these irradiation conditions. In order to get better statistics the data from 2015 to 2016 were grouped yielding an average α for the period. It can be seen that the values of α are close to zero, indicating an epithermal neutron field approaching the ideal spectrum. As a result, $Q_0(\alpha)$ approaches Q_0 according to equation (7). The parameter $\boldsymbol{a}$ from equation (3) corresponds to the value of Y_i when $ln\bar{E}_{r,i}$ goes to zero, and resulted 25.84(3).

The k_0 results are presented in Table 4 for methods A and B. The number inside parentheses corresponds to the uncertainty in the last digits (one standard deviation). There is a good agreement among the two methods within the corresponding uncertainties. A weighted average of the two methods has been evaluated considering the correlations among the methods.

The comparison between the present values for $\boldsymbol{k_0}$ and the literature was performed by applying the Zeta Score factor (ISO 13528, 2015) between each pair of data points. This factor is defined by:

$$Zeta = \frac{X_i - X_{ref}}{\sqrt{u_X^2 + u_{ref}^2}} \quad (9)$$

where $\boldsymbol{X_i}$ corresponds to the $\boldsymbol{k_0}$ value from the present work and $\boldsymbol{X_{ref}}$ from the literature; $\boldsymbol{u_X}$ and $\boldsymbol{u_{ref}}$ correspond to the uncertainties in each parameter (one standard deviation).

The Zeta Score factors for the $\boldsymbol{k_0}$ results are shown in Table 5. Agreement was considered when the absolute value of this factor was below 3.0 (99% confidence interval).

In the case of ^{75}Se, the average values from the present work agree with the k_0-database value (2019), Jaćimović and Stibilj (2010), except marginally at 400 keV, Sneyers and Vermaercke (2014) and Lin and Von Gostomski (2013), but disagrees with De Corte and Simonits (2003) at 121, 136 and 264 keV and agrees only marginally at 279 and 400 keV.

For ^{114m}In, the average values agree well with Arboccò et al. (2014), but disagree with De Corte and Simonits (2003) at 725 keV, and agree only marginally for the other energies.

For ^{187}W the average values from the present work agree marginally with De Corte and Simonits (2003), which corresponds to the k_0 database, and is the only data available in the literature, suggesting that new measurements are desirable. It can be pointed out that the value for 625.51 keV has been measured in the present work for the first time.

For ^{192}Ir the average value agrees reasonably well with the first value given by Chilian et al. (2014) - obtained from measurements carried out in the research reactor of Ecole Polytechnique Montreal, but not so well with the second value given by Chilian et al. (2014) - obtained from measurements carried out in the research reactor of SCK•CEN, except at 308 keV; the present work agrees with the values from k_0 -database value (2019) and from Stopic and Bennett (2014), the latter only marginally at 468 keV.

The Q_0 results are presented in Table 6. The reported values correspond to the weighted average of all gamma transitions, applying covariance analysis. The Zeta Score factor for each pair was also applied for the comparisons and are shown in Table 7.

For ^{75}Se the value agrees well with all other data from the literature, but only marginally with Jaćimović and Stibilj (2010). The reported value by Trkov et al. (2015) was not obtained experimentally, but calculated from tabulated thermal cross section and resonance integral values. For ^{114m}In, the result agrees well with De Corte and Simonits

Table 7
Comparison between the Q_0 and the literature, applying the Zeta score parameter. Agreement was considered for Zeta below 3.0 (99% confidence interval). The references are indicated by a superscript and are described at the bottom of the table.

Reaction	Zeta Score between pairs of Q_0 values obtained in this work and taken from the literature (indicated as superscript)					
^{74}Se(n,γ) ^{75}Se	0.54[a]	2.45[b]	0.45[c]		0.21[e]	
^{113}In(n,γ)^{114m}In	0.69[a,c]			0.15[d]	−5.30[e]	1.28[f]
^{186}W(n,γ)^{187}W	−1.26[a,c]				0.25[e]	
^{191}Ir(n,γ)^{192}Ir	−0.94[g1]	1.39[g2]	−0.03[c]			

[a] De Corte and Simonits (2003).
[b] Jaćimović and Stibilj (2010).
[c] k0 database (2019).
[d] Sneyers and Vermaercke (2014).
[e] Trkov et al. (2015).
[f] Arboccò et al. (2014).
[g1] Chilian et al. (2014) – *Polytechnique*.

Table 8
Average values of k_0 and Q_0 and the corresponding Correlation Matrix. The numbers inside parentheses correspond to uncertainties in the last digits (one standard deviation).

Reaction	Parameter	Energy (keV)	Value	Correlation Matrix (x 1000)							
^{74}Se(n,γ) ^{75}Se	k_0	121.12	2.17(4) × 10^{-3}	**1000**							
		136.00	7.52(13) × 10^{-3}	**962**	**1000**						
		264.66	7.58(12) × 10^{-3}	**866**	**834**	**1000**					
		279.54	3.19(5) × 10^{-3}	**896**	**829**	**945**	**1000**				
		400.66	1.51(4) × 10^{-3}	**901**	**809**	**853**	**927**	**1000**			
	Q_0	Average	11.3(6)	**−29**	**−30**	**−51**	**−44**	**−29**	**1000**		
^{113}In(n,γ)^{114m}In	k_0	190.30	1.021(16) × 1-0^{-3}	**400**	**383**	**549**	**519**	**433**	**−113**	**1000**	
		558.40	2.73(5) × 10^{-4}	**515**	**503**	**620**	**596**	**533**	**−134**	**872**	**1000**
		725.20	2.73(5) × 10^{-4}	**524**	**513**	**617**	**596**	**539**	**−136**	**842**	**964**
	Q_0	Average	24.7(6)	**−57**	**−58**	**−100**	**−87**	**−55**	**242**	**−312**	**−252**
^{186}W(n,γ)^{187}W	k_0	479.53	3.22(8) × 10^{-2}	**290**	**275**	**393**	**372**	**313**	**−83**	**430**	**368**
		551.53	7.31(18) × 10^{-3}	**322**	**310**	**405**	**388**	**337**	**−82**	**427**	**381**
		618.77	9.15(22) × 10^{-3}	**312**	**299**	**400**	**382**	**330**	**−84**	**426**	**376**
		625.51	1.58(5) × 10^{-3}	**434**	**434**	**404**	**402**	**404**	**−67**	**347**	**383**
		685.77	3.97(9) × 10^{-2}	**286**	**272**	**389**	**368**	**310**	**−85**	**425**	**365**
		772.89	5.98(15) × 10^{-3}	**317**	**304**	**399**	**382**	**333**	**−85**	**422**	**376**
	Q_0	Average	12.9 (6)	**−20**	**−20**	**−38**	**−32**	**−18**	**122**	**−59**	**−36**
^{191}Ir(n,γ)^{192}Ir	k_0	295.96	1.169(18)	**501**	**481**	**701**	**661**	**556**	**−173**	**575**	**610**
		308.46	1.186(18)	**499**	**479**	**697**	**656**	**555**	**−162**	**575**	**611**
		316.51	3.37(5)	**489**	**469**	**697**	**655**	**549**	**−172**	**576**	**607**
		468.07	1.949(31)	**495**	**475**	**697**	**656**	**551**	**−170**	**574**	**606**
	Q_0	Average	3.77(11)	**−192**	**−190**	**−306**	**−282**	**−198**	**551**	**−146**	**−175**

Reaction	Correlation Matrix (x 1000)													
^{74}Se(n,γ) ^{75}Se														
^{113}In(n,γ)^{114m}In														
	1000													
	−246	**1000**												
^{186}W(n,γ)^{187}W	**357**	**−68**	**1000**											
	372	**−68**	**948**	**1000**										
	367	**−69**	**950**	**953**	**1000**									
	389	**−55**	**775**	**830**	**817**	**1000**								
	354	**−70**	**952**	**948**	**949**	**776**	**1000**							
	368	**−71**	**947**	**952**	**952**	**829**	**947**	**1000**						
	−35	**216**	**−314**	**−311**	**−315**	**−249**	**−318**	**−316**	**1000**					
^{191}Ir(n,γ)^{192}Ir	**601**	**−99**	**446**	**445**	**444**	**368**	**443**	**441**	**−45**	**1000**				
	603	**−97**	**447**	**446**	**446**	**371**	**444**	**442**	**−45**	**927**	**1000**			
	597	**−97**	**447**	**444**	**443**	**358**	**444**	**440**	**−45**	**927**	**925**	**1000**		
	596	**−100**	**445**	**442**	**442**	**362**	**441**	**438**	**−46**	**929**	**927**	**928**	**1000**	
	−176	**402**	**−110**	**−109**	**−111**	**−89**	**−113**	**−113**	**212**	**−87**	**−88**	**−88**	**−84**	**1000**

(2003), which corresponds to the value from the k0 database (2019) and with Arboccò et al. (2014) but disagrees with Trkov et al. (2015). For ^{187}W, the result agrees with all data from the literature, namely: Trkov et al. (2015) and De Corte and Simonits (2003). The latter corresponds to the value from the k0 database (2019). For ^{192}Ir, there are two values in the literature taken from the same reference (Chilian et al., 2014) and another one from the k0 database (2019). The present result agrees with all of these data, especially with the data from the k0 database (2019).

Table 8 shows the values together with the total uncertainties in k_0 and Q_0 and the corresponding correlation matrix between all measured data pairs. This information may be required when using the present results for other applications. The correlation factor between k_0 values is positive. This can be explained considering that several parameters used for the comparator (Au) are the same and contribute with identical components to equations (1) and (2). For the same target and different gamma-ray energies, the correlation is higher due to the presence of common components, e.g. the activity. For different targets the correlations are lower. Considering equation (6), the correlation factors between pairs of Q_0 values are also positive. The correlation between k_0 and Q_0 values are negative. In this case, for k_0 the target component appears in the numerator and the comparator component appears in the denominator. For Q_0 these positions are inverted. Therefore, any variation in a given parameter tends to change k_0 and Q_0 in opposite directions, resulting in a negative correlation. The complete correlation matrices among all partial parameters shown in Tables 4 and 6 are too extensive to be presented here and are reported in a PhD thesis (Barros, 2018).

4. Conclusions

The k_0 and Q_0 factors were measured for ^{74}Se, ^{113}In, ^{186}W and ^{191}Ir targets near the IEA-R1 research reactor core at a location where the parameter α is very close to zero, corresponding to an almost ideal epithermal neutron field. Several comparisons were made with data from the literature showing similarities and differences. The $\boldsymbol{k_0}$ value for the energy 625.51 keV of ^{187}W has been measured in the present work, for the first time.

Acknowledgment

The authors are indebted to the National Council for Scientific and Technological Development (CNPq, Brazil), for partial support of the present research work (contract number PQ-302747/2014-1) and to the National Nuclear Energy Commission (CNEN, Brazil) for sponsoring the fellowship of one of the authors (public notice number 04/2014).

Appendix A. Supplementary data

Supplementary data to this article can be found online at https://doi.org/10.1016/j.apradiso.2019.108846.

References

Arboccò, F.F., Vermaercke, P., Smits, K., Sneyers, L., Strijckmans, K., 2014. Experimental determination of k_0, Q_0 factors, effective resonance energies and neutron cross-sections for 37 isotopes of interest in NAA. J. Radioanal. Nucl. Chem. 302, 655–672.

Barros, L.F., 2018. Determinação de k_0 *e* Q_0 para as reações ^{74}Se(n, γ) ^{75}Se, ^{113}In(n, γ) ^{114m}In, ^{186}W(n, γ) ^{187}W e ^{191}Ir(n, γ)^{192}Ir. PhD Thesis, in Portuguese. Universidade de São Paulo, São Paulo. https://doi.org/10.11606/T.85.2018.tde-21092018-143710.

Chilian, C., Sneyers, L., Vermaercke, P., Kennedy, G., 2014. Measurement of k_0 and Q_0 values for iridium isotopes. J. Radioanal. Nucl. Chem. 300, 609–613.

De Corte, F., 1987. The k_0-standardization method: a move to the optimization of neutron activation analysis. PhD Thesis. Rijksuniversiteit Gent.

De Corte, F., Simonits, A., 2003. Recommended nuclear data for use in the k_0 standardization of neutron activation analysis. Atomic Data Nucl. Data Tables 85, 47–67.

Dias, M.S., Cardoso, V., Vanin, V.R., Koskinas, M.F., 2004. Combination of nonlinear function and mixing method for fitting HPGe efficiency curve in the 59–2754 kev energy range. Appl. Radiat. Isot. 60, 683–687.

Dias, M.S., Cardoso, V., Koskinas, M.F., Yamazaki, I.M., 2010. Determination of the neutron spectrum shape parameter α in k_0 NAA methodology using covariance analysis. Appl. Radiat. Isot. 68, 592–595.

Dias, M.S., Cardoso, V., Koskinas, M.F., Yamazaki, I.M., Semmler, R., Moralles, M., Zahn, G.S., Genezini, F.A., de Menezes, M.O., Figueiredo, A.M.G., 2011. Measurements of k_0 and Q_0 values for ^{64}Zn(n,γ)^{65}Zn and ^{68}Zn(n,γ)^{69m}Zn reactions with covariance analysis. Appl. Radiat. Isot. 69, 960–964.

Firestone, R.B., Kellett, M.A., 2008. Second Research Coordination Meeting on Reference Database for Neutron Activation Analysis - Summary Report. Berkeley, CA.

ISO 13528, 2015. Statistical methods for use in proficiency testing by interlaboratory comparison. https://www.iso.org/obp/ui/#iso:std:iso:13528:ed-2:v2:en.

Jaćimović, R., Stibilj, V., 2010. Determination of Q_0 and k_0 factors for ^{75}Se and their validation using a known mass of Se on cellulose. Nucl. Instruments Methods Phys. Res. Sect. A Accel. Spectrometers, Detect. Assoc. Equip. 622, 415–418.

k0 database, April 2019. http://www.kayzero.com/k0naa/k0naaorg/Nuclear_Data_SC/Entries/2019/4/15_Update_of_k0-database_Ba-131_files/k0_database_2019_04_04.xls.

Kodeli, I., Trkov, A., July 2007. Validation of the IRDF-2002 dosimetry library. Nucl. Instruments Methods Phys. Res. Sect. A Accel. Spectrometers, Detect. Assoc. Equip. 577 (3), 664–681.

Lin, X., Von Gostomski, C.L., 2013. Determination of the k_0-values for ^{75}Se, ^{110m}Ag, ^{115}Cd–^{115m}In, ^{131}Ba, and ^{153}Sm by irradiation in highly thermalized neutron flux. J. Radioanal. Nucl. Chem. 295, 1921–1925.

Sneyers, L., Vermaercke, P., 2014. Determination of Q_0 and k_0 factors for ^{75}Se. J. Radioanal. Nucl. Chem. 300, 599–604.

Stopic, A., Bennett, J.W., 2014. Measurement of k_0 values for caesium and iridium. J. Radioanal. Nucl. Chem. 300, 593–597.

Trkov, A., 2016. MATSSF- material attenuation self shielding factor. WWW Document. www-nds.iaea.org/naa/matssf/.URL.www-nds.iaea.org/naa/matssf 08-Sep-2016.

Trkov, A., Kaiba, T., Žerovnik, G., Revay, Z., Firestone, R., Jaćimovic, R., Radulovic, V., 2015. Supplementary Data for Neutron Activation Analysis. INDC (NDC)-0693.